

CENTRAL ASIAN JOURNAL OF THEORETICAL AND APPLIED SCIENCE

https://cajotas.casjournal.org/index.php/cajotas

Volume: 08 Issue: 01 | January 2027 ISSN: 2660-5317

Article

Theoretical Investigation of Proton Electronic Stopping Power and CSDA Range in Human Intestine, Larynx, and Skin Tissues Using Hartree–Fock–Roothaan Wave Functions

Malik Abdullah Atheeb[1]

1. Education Ministry, Education General Rusafa, 3 Direction, Baghdad, Iraq

* Correspondence: malk84419@gmail.com

Abstract: This study presents a theoretical investigation of the electronic stopping power and continuous slowing down approximation (CSDA) range of protons in three human biological tissues: intestine, larynx, and skin. The electronic energy loss of incident protons was calculated as a function of their kinetic energy using the theoretical stopping-power model. Furthermore, the CSDA method was employed to determine the penetration range of protons in the investigated tissues. The results demonstrate that the electronic stopping power generally decreases with increasing proton energy, indicating a reduction in energy loss per unit mass thickness at higher projectile energies. In contrast, the calculated CSDA range increases with increasing incident proton energy, reflecting the greater penetration capability of high-energy protons. These trends demonstrated inversely relative between stopping power and range of proton penetration. The comparative investigation of the three biological tissues provides theoretical insight into proton–matter interactions, energy-transfer mechanisms, and radiation penetration in biological materials. The findings may contribute to a better understanding of proton transport and energy deposition in biological tissues and provide a theoretical basis for further investigations related to proton radiation applications.

Keywords: Proton, Tissue, Hartree-Fock-Roothaan , CSDA range, Stopping power

Citation: Atheeb, M. A. Theoretical Investigation of Proton Electronic Stopping Power and CSDA Range in Human Intestine, Larynx, and Skin Tissues Using Hartree–Fock–Roothaan Wave Functions. Central Asian Journal of Theoretical and Applied Science 2027, 8(1), 124-135

Received: 16th Aug 2026
Revised: 18th Sep 2026
Accepted: 15th Oct 2026
Published: 19th Nov 2026

Copyright: © 2027 by the authors. Submitted for open access publication under the terms and conditions of the Creative Commons Attribution (CC BY) license (https://creativecommons.org/licenses/by/4.0/)

1. Introduction

In physics, "stopping power" is defined as the rate at which a material absorbs the kinetic energy of a charged particle—such as alpha particles or electrons—due to its interaction with the material, causing the particle to lose its kinetic energy. This property is of great importance in fields such as radiation protection, ion implantation, and nuclear medicine [1]. Knowing the stopping power of organic biomaterials towards protons is of critical importance in varity areas of basic and applied work, such as radiobiology, biomedical applications, and radiation therapy [2]. Calculations of the "stopping power" of charged particles in matter are a subject of long-standing interest, both experimentally and theoretically, in the fields of radiation physics, medicine, chemistry, microdosimetry, biology, and proton therapy [3]. Because of the great importance of the concept of the "stopping power" of charged particles as they pass through matter - particularly in the field of radiation damage physics - this topic has received great attention for about a hundred years; when charged particles penetrate a material, they lose their energy mainly through two processes: the excitation and ionization of atoms [4]. Furthermore, Alpha particles are emitted by many heavy nuclei, particularly those in natural radioactive decay series. Although they have low penetration power, they lose energy through excitation

and ionization when passing through matter. These processes can affect biological tissues, making alpha particles useful in cancer radiotherapy but also posing occupational radiation hazards to nuclear reactor personnel[5]. The stopping power depends on more than one factor, including: the target material, the speed of the projectile particle, and its charge [6]. The stopping power arises from the collision of charged particles with the nuclei of the target material's atoms (known as nuclear stopping power) and with its electrons (known as electronic stopping power). At low energies, nuclear stopping power can be neglected [7]. Electronic stopping power is typically defined as the total power loss at low power levels [8].Proton beams are used in radiation therapy for the effective treatment of tumors. The precise determination of the proton radiation dose depends on the availability of comprehensive information about the "stopping power" and "range" values of the protons within the target material[9]. In particular, stopping power and range data must be known to characterize dummy materials and radiation detector materials[10].Many researchers are studied the stopping power of protons in various organic materials, but data on stopping power and range in tissues are scarce. Therefore, there is a need for information on the stopping power and range of protons in body tissues, particularly in proton therapy[11]. When heavy ions travel through matter at velocities below the speed of light, their electronic stopping power is influenced by electron capture, ion excitation and ionization, target-atom excitation and ionization, interactions with free electrons, and collective effects such as polarization. These processes determine energy deposition in biological tissues and are essential for evaluating the therapeutic effectiveness of ion radiation and its potential damage to surrounding healthy tissues[12]. The use of protons in radiation therapy is a promising way to spare healthy tissues, thanks to their distinctive depth-dose curve; this makes knowing the "stopping power" (SP) of protons in biological tissues extremely important[13].Proteins are vitally important organic compounds. Their functions and physical structure are subjects of well-established experimental and theoretical interest. Amino acids are the basic building blocks of proteins, and their sequences contribute to their functions. Therefore, predicting the proton bands of amino acids or proteins is of fundamental importance in radiobiology and biomedical applications[14]. In this work, systematic calculations of the ange and electronic stopping power of charged particle is protonfor larger than 1 MeV protons in a group of in some of human tissue have been performed. The deceleration process of protons—as charged particles—and their capacity for electron loss have been studied theoretically. These calculations are based on a Bethe-type formulation to calculate the capacity for energy loss, taking into account the average excitation energy of the target material and the effective charge of the particle. The aim of this work is to present the proton stoping power of the skin, Larynx and intestine tissues because of their importance in radiation biology.

2. Materials and Methods

The electronic stopping power of a proton's passage through a material is determined by its interactions with the electrons of the target atoms. These interactions include atomic excitation, ionization, and electron density polarization. The energy loss depends on the projectile's velocity, the target's electronic structure, and the material's average excitation energy[15].The interaction potential between the incident proton and the target atom can be expressed as[16]

$$U(x,y,D) = \frac{Ze^2}{D} - \sum_{i=1}^{Z^*} \frac{e^2}{|D-y_i|} \qquad (1)$$

Where e is electron charge , Z is nuclear charges , Z^* the target efficient charge , D is the projectile location depending on the target mass center, y_i target location vector i electron regarding the target mass center . The electronic stopping power is calculated using the Bethe equation and can write as [17]:

$$\frac{dE}{dx} = \left(\frac{e^2}{4\pi\varepsilon}\right)\left[\frac{N_o Z^2 \rho(T+mc^2)}{137 m^2 c^4 A}\right][4ln\frac{2(T+mc^2)}{mc^2 mc^2} - \frac{4}{3}] \qquad (2)$$

Where T is electronic kinetic energy , c is speed light .The energy loss for proton using Eq.(1) and Eq.(2) in the procedure depicted to get the energy loss for proton[18].

$$(\frac{dE}{dx}=)_{electron}=\frac{4\pi e^4}{m_e c^2\gamma^2}q^*\ln(\frac{b_{max}}{b_{min}}) \quad (3)$$

Where e is elementary charge , m_e is electron mass,c is speed of light , $\gamma=\frac{v}{c}$ is relativistic Lorentz factor (velocity of proton in units of light velocity), q^* is effective charge factor , b_{max} and b_{min} are transfer of minimum and maximum parameters from libeller to target which are given by[19].

$$b_{max}=\frac{2m_e v}{\hbar} \quad , \; b_{min}=\frac{\alpha^*}{\hbar v} \quad (4)$$

It should be noted that the stopping power of the falling particle in both expression s Eq.() an dEq.() is inversely proportional to the square of the particle's speed and directly proportional to the square of its charge. Also, the loss of energy does not depend on the mass of the charged particle, but rather on the properties of the target material, namely: density, atomic number, atomic mass, and average excitation energy [20]. The average of efficient excitement energy α^* for target can be given as [19-21] .

$$ln\alpha^*=\frac{1}{q}\int_{r_\circ}^{\infty}\ln[B\hbar W_p(r)]4\pi r^2\rho(r)dr \quad (5)$$

Where $\rho(r)$ is density of electric charge , B is an amenable parameter, r distance from nucleus , $W_p(r)$ is hesitance of plasma and $r_\circ$ critical dimension from atom center until determine the efficient charge which by using the stripping standard for Boher .However ,the effective charge factor can be formulated using integral given by [21].

$$q^*(E)=\int_{r_\circ}^{\infty}4\pi r^2\rho(r)dr \quad (6)$$

The density of electric charge $\rho(r)$ is depicted as [22]

$$\rho(r)=\sum_\delta|U_\delta(r)|^2 \quad (7)$$

Where $U_\delta(r)$ atomic wave function of δ orbital via applied the atomic wave function for Hartrre –Fock –Roothoan HFR [23] .The time-independent particle model (HFRS) relies on the Hartree-Fock method, which is used to solve the Schrödinger equation for electrons moving at the nuclear potential. This process involves iterating the calculations until the resulting electron charge density approaches the initial charge density. Solutions to the Hartree-Fock equations (HFRS) are defined as those in which the electron orbitals are represented by Slater-type orbitals,it is represented as

$$U_\delta(r)=\sum_{i=1}^{m}g_i h_i(r) \quad (8)$$

Where is g_i is coefficient of orbital expansion and $h_i(r)$ represent orbital of Starter –type which can write by

$$h_i(r)=M_i r^{m_{i-1}}e^{\gamma_i r} \quad (9)$$

where M_i is constant of normalization and m_i number of the principal quantum.Therefore, the range is inherently an average value, defined for a beam of particles, not individual particles. By convention, this means that half of the protons incident on the absorbing material stop, although in some cases this may be interpreted as half of the protons continuing their motion until they reach the edge of the range. The range of proton can be calculated using The proton range can be calculated using the Continuous Slowing Down Approximation (CSDA) method. The range of protons due to this method can compute from the integrating over the initial and final fallen particles energy to energy loss invers which given by[24].

$$R=\rho\int_{E_f}^{E_\circ}\frac{dE}{(\frac{dE}{dx}=)_{electron}} \quad (10)$$

Where $E_\circ$ is initial energy and E_f is final energy for charged particle that fallen in target, only we have taken the electronic energy loss in our computations, range of CSDA has been computed by

3. Results

The racial composition of most body tissues shows marked variations between individuals of the same age group.Furthermore, factors such as metabolism, dietary habits, sex, and health status can influence these compositions. Some of these differences are also attributed to variations in the experimental methodologies and techniques employed by researchers. Consequently, data related to radiation reactions may contain errors. In the preceding theory, proton energy loss was approximated as a continuous process based on the mean stopping power, neglecting individual energy-loss fluctuations. Although this approximation is suitable for many clinical calculations,

energy and range straggling significantly influence the proton Bragg curve and dose distribution. Therefore, considering range straggling is essential for understanding proton dose profiles [25].Calculating the stopping power of electrons as they pass through matter is similar to calculating it for heavy charged particles. The interaction of incoming electrons with the electrons of atoms—which leads to the excitation or ionization of the atoms—can be calculated using Bethe's theory; this is called collisional stopping power. Additionally, electrons gain acceleration when they are within the Coulomb field of the nucleus, resulting in the emission of electromagnetic radiation known as Bremsstrahlung; the stopping power associated with this process is called radiative stopping power. The present study investigates the electronic stopping power and CSDA range of incident protons in human intestine, larynx, and skin tissues. The electronic energy loss was calculated using Eq. (2), and the corresponding proton ranges were determined using the continuous slowing down approximation (CSDA) method. The stopping power calculation and values of range evaluate as functions of energy of protons for intestine presents in Table 1, for larynx in Table 2, and for skin tissue in Table 3.The proton stopping power as well as CSDA range calculation exhibited a more dependent on the energy of incident protons. As shown data in tables 1 ,2 and 3, the stopping power was decreasing with increased energy of protons, it indicats a reduced in the energy transport by protons to the target per unit mass and path length. At low energies, the stopping power is relatively high, reaching 207.294 at 1.007 MeV, and decreases to 4.711 at 126.579 MeV. This characteristics behavior indicated that lowest energy protons undergoing greater energy loss than highest energy protons.However, the stopping power decreased at higher energies to reach 0.567 at 678.672 MeV. Results indicates to the energy dependent of the proton– interaction as well as energy-transfer.

Table 1. Characteristics of stopping power and range of proton with energy in Intestine

Energy(MeV)	SP(MeV/g/cm²)	Energy(MeV)	Range (cm)
1.007	207.294	50	2.31
1.191	191.878	59.9	2.82
1.389	173.957	71.3	4.36
1.576	160.289	84.2	5.9
1.972	137.205	89.5	6.92
2.505	116.633	97.1	7.69
3.274	95.174	106	9.23
5.15	67.544	115	10.8
7.242	51.877	124	12.6
11.102	36.926	132	14.1
18.563	24.375	140	15.4
28.922	16.985	147	16.9
48.434	11.174	156	19
77.708	6.268	163	20.5
126.579	4.711	171	22.6
163.837	2.648	179	24.6
203.246	3.175	185	26.2
286.794	1.828	191	27.7
467.256	1.114	199	29.7
678.672	0.567	206	31.8

The CSDA range calculation was increased continuously via increased proton energy. Furthermore ,the range proton was increased from 2.31 cm at 50 MeV to 46.2 cm at 248 MeV. This characteristic has been consistent due to physical expectated that higher-energy protons penetrated deeper into the target when losing more energy. The range of protons was increased and becomes more pronounced with high energies, demonstration

the strong dependent of penetration depth on proton energy.The characteristics of electron stopping power with energy in Intestine as shown in figure 1.

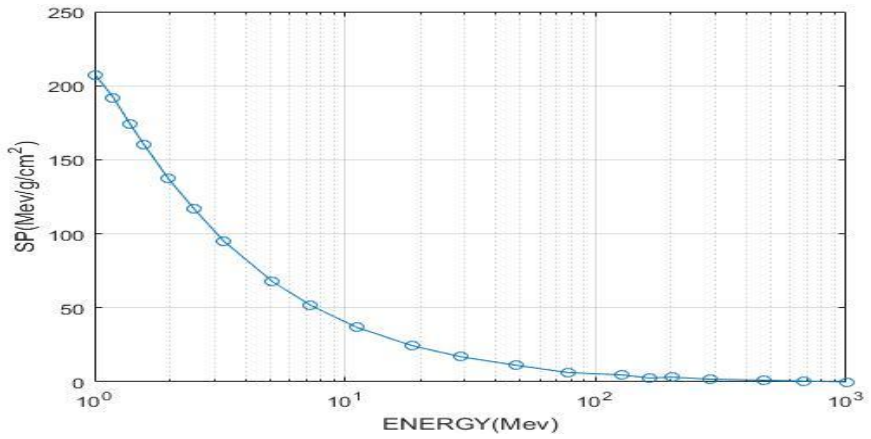

Figure 1. The electronic stopping power with Energy in intestine

Figure 1 showes the inverse relationship between stopping power and proton range is particularly evident in the results. Protons has lower energies would be exhibited high stopping powers as well as short penetration distances comparing with high energy protons exhibited low stopping powers with long ranges. These indicates demonstrated the important of proton energy in determination energy deposited with penetration depth in tissues. Consequently, the calculated stopping-power and range values provide useful information for understanding proton transport and energy deposition in intestine, larynx, and skin tissues.

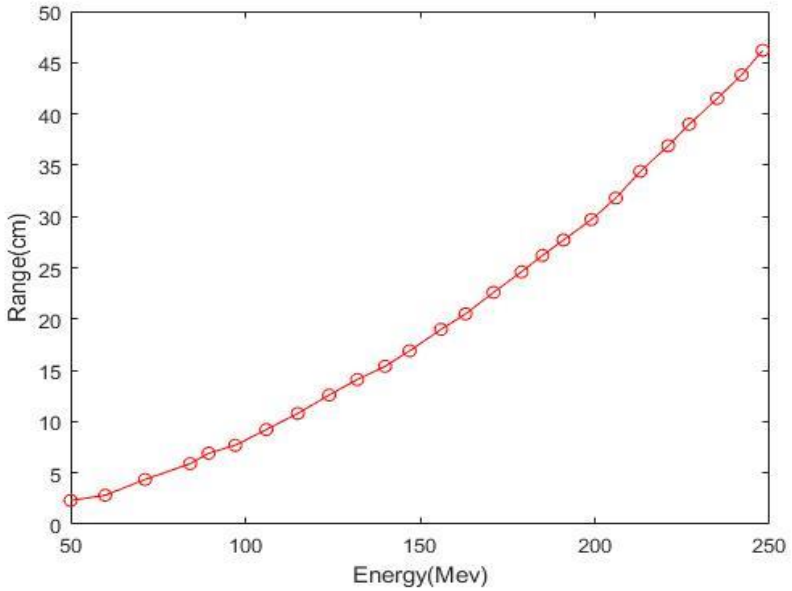

Figure 2. Range as founction of energy in intestine.

Figure 2 illustrates the change in the continuous slowing approximation in range (CSDA) of protons due to the kinetic energy in human intestinal tissue. At 50 MeV, the calculated range is 2.31 cm, increasing to 2.82 cm at 59.9 MeV and 4.36 cm at 71.3 MeV. As increasing in proton energy, the range can be rised to 9.23 cm with 106 MeV and 15.4 cm with 140 MeV. At higher energies, the range reaches 22.6 cm at 171 MeV and 31.8 cm at 206 MeV. This increasing trend can be attributed to the greater initial kinetic energy of high-energy protons, which enables them to penetrate deeper into the tissue before losing their energy through interactions with the target electrons. Results indicated a non-linear relationship between protons energies and range .The range increased progressively over the investigated energy interval. Results data showes a demonstrated that l kinetic energy

was vital parameter govern proton depth in human intestine tissue. The calculated CSDA ranges may provide useful theoretical information for understanding proton transport and energy deposition in biological tissues, particularly in applications involving proton radiation and particle therapy.

Table 2: Stopping power and range characteristics of proton with energy in Larynx.

Energy(MeV)	SP(MeV/g/cm2)	Energy(MeV)	Range (cm)
1	207.303	0.979	8.915
1.252	183.753	29.662	10.061
1.613	154.272	70.631	12.892
2.359	117.24	91.111	15.143
3.306	91.157	134.109	21.876
4.834	66.765	174.02	31.392
6.681	51.636	231.313	47.611
10.334	35.678	259.953	57.114
15.109	26.455	280.414	63.265
26.153	16.409	299.846	69.972
43.398	10.572	320.292	78.908
79.47	5.59	341.76	88.403
137.56	3.129	366.296	99.015
234.56	2.351	399.011	112.979
461.266	1.591	416.381	122.47
173.445	1.644	444.986	138.657

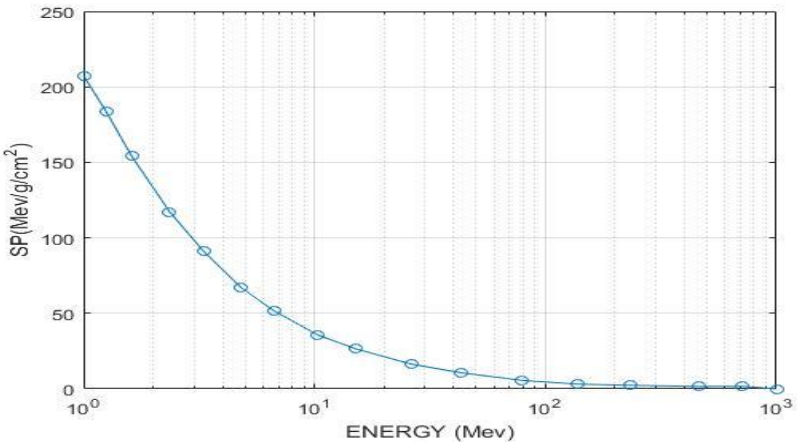

Figure 3. Electronic stopping power as founction of energy in Larynx

Electronic stopping power calculations of protons in larynx tissue exhibited a decreasing with increasing proton energy, as showing in Table 2. At low proton energies, the stopping power is relatively high, reaching 207.303 MeV·cm²/g at 1 MeV. As the proton energy increases, the stopping power decreases to 183.753 MeV·cm²/g at 1.252 MeV and 154.272 MeV·cm²/g at 1.613 MeV. This reduce continues due to increase energy to reach 91.157 MeV·cm²/g at 3.306 MeV and 51.636 MeV·cm²/g at 6.681 MeV.

Figue3 At higher proton energies, the stopping power decreases further, reaching 26.455 MeV·cm²/g at 16.409 MeV and 16.409 MeV·cm²/g at 26.153 MeV. These results indicate that low-energy protons deposit a greater amount of energy per unit mass and path length in the larynx tissue compared with high-energy protons. This behavior is associated with the dependence of proton–electron interactions and energy-transfer mechanisms on projectile velocity.

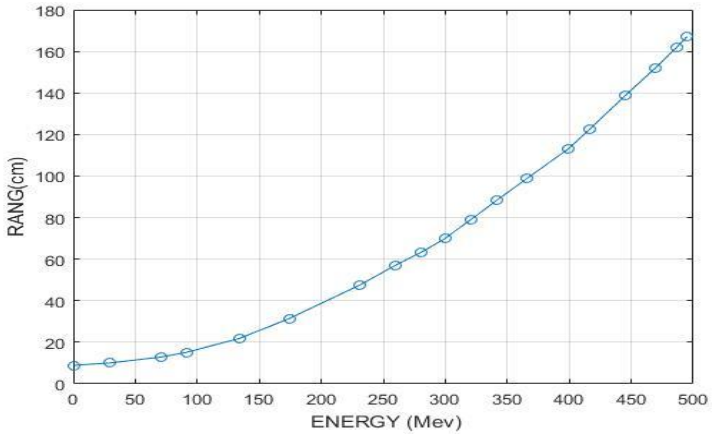

Figure 4. The Range with Energy in Larynx

Table 2 and figure 4 show the calculated CSDA range shows an increasing trend with increasing initial proton energy. As indicated in Table 2, the proton range increases from 8.915 cm at 0.979 MeV to 10.061 cm at 1.252 MeV and 12.892 cm at 1.613 MeV. With further increases in proton energy, the range reaches 21.876 cm at 3.306 MeV and 31.392 cm at 4.834 MeV.

Figure 4 indicates that proton range increased considerably at high energies and reaches to (47.611 cm) at 6.681 MeV, (57.114 cm) at 10.334 MeV, and (69.972 cm) at 15.109 MeV. On the other hand ,the range increased to (88.403 cm) at 26.153 MeV and (112.979 cm) at 43.398 MeV.

At the highest reported energy of 138.657 MeV, the range calculation is 444.986 cm.

This indicates that high-energy protons have the ability to penetrate deeper into laryngeal tissues because they possess a large amount of kinetic energy, requiring a longer distance to lose their energy through interactions between the protons and the target tissue. The results show an inverse relationship between the stopping power and the range of protons .When the energy of protons is low, they exhibit a higher stopping power and lose their kinetic energy at a faster rate. However, high energy protons exhibit low stopping power with large range distances into the tissue. These results determine an important amount of proton energy in relation to energy deposition and the extent of its penetration into laryngeal tissues.Calculating of stopping power and continuous CSDA-range provides additional knowledge that helps in understanding how protons are transported and their energy is deposited within tissues, which serves applications of proton radiotherapy.

Table 3. The characteristics of proton stopping power and rang as founction of energy in Skin

Energy(MeV)	SP(MeV/g/cm2)	Energy(MeV)	Range (cm)
1.001	209.831	0.097	9.524
1.269	184.434	27.655	10.239
1.564	161.579	57.266	12.086
1.928	138.725	107.32	17.408
2.411	117.548	135.939	22.05
3.146	96.351	174.797	30.111
4.343	75.126	213.683	40.973
6.348	56.402	243.368	50.103
9.803	40.177	274.08	59.799
15.642	27.31	297.63	67.774
26.75	17.778	325.297	79.133
48.421	9.904	349.891	89.355
74.01	7.169	370.386	97.873

Energy(MeV)	SP(MeV/g/cm2)	Energy(MeV)	Range (cm)
108.42	4.455	387.809	105.254
150.212	3.453	401.132	110.931
196.42	2.48	420.624	121.124
264.377	1.492	442.168	132.449
376.618	1.319	463.718	144.335
528.971	1.153	481.157	153.396
682.464	1.029	500.655	164.149

The calculated electronic stopping power (SP) in table 3 exhibits a clear decreasing trend with increasing incident proton energy, as presented in the table. At low energies, the stopping power reaches a maximum value of 209.831 MeV·cm²/g at 1.001 MeV. As the proton energy increases, the stopping power decreases to 184.434 MeV·cm²/g at 1.269 MeV and 161.579 MeV·cm²/g at 1.564 MeV. This reducedcontinues to reach 96.351 MeV·cm²/g for 3.146 MeV and 56.402 MeV·cm²/g for 6.348 MeV.

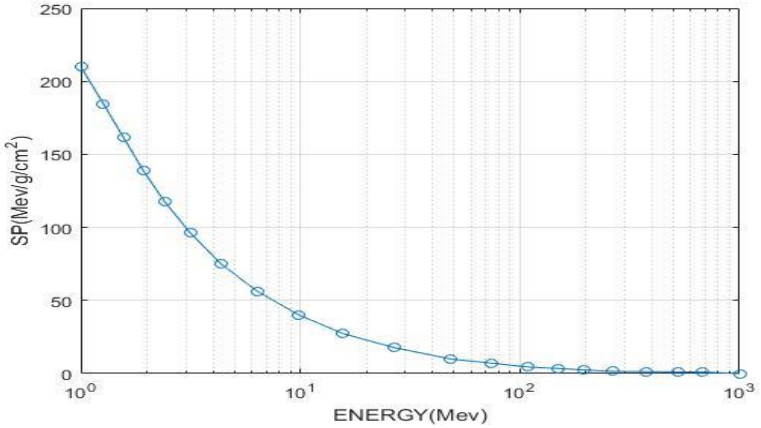

Figure 5. The electronic stopping power with Energy in Skin

Figure 5 show that at higher proton energies, the stopping power decreases further, reaching 27.31 MeV·cm²/g at 17.778 MeV and 9.904 MeV·cm²/g at 48.421 MeV. At 164.149 MeV, the stopping power reaches 1.029 MeV·cm²/g. This behavior indicates that low-energy protons experience greater energy loss per unit mass thickness than high-energy protons. The decreasing trend is associated with the dependence of energy transfer during proton–electron interactions on the projectile velocity. The calculated continuous slowing down approximation (CSDA) range increases progressively with increasing initial proton energy. At 0.097 MeV, the calculated range is 9.524 cm, increasing to 10.239 cm at 27.655 MeV and 12.086 cm at 57.266 MeV. With further increases in proton energy, the range reaches 17.408 cm at 107.32 MeV and 22.05 cm at 135.939 MeV.At higher energies, the proton range increases considerably, reaching 30.111 cm at 174.797 MeV, 40.973 cm at 213.683 MeV, and 50.103 cm at 243.368 MeV. The range continues to increase, reaching 67.774 cm at 297.63 MeV and 89.355 cm at 349.891 MeV. At the highest reported energy of 500.655 MeV, the calculated range reaches 164.149 cm.This increasing behavior demonstrates that high-energy protons can penetrate deeper into the biological tissue because they possess greater initial kinetic energy and require a longer distance to lose their energy through interactions with the target medium.

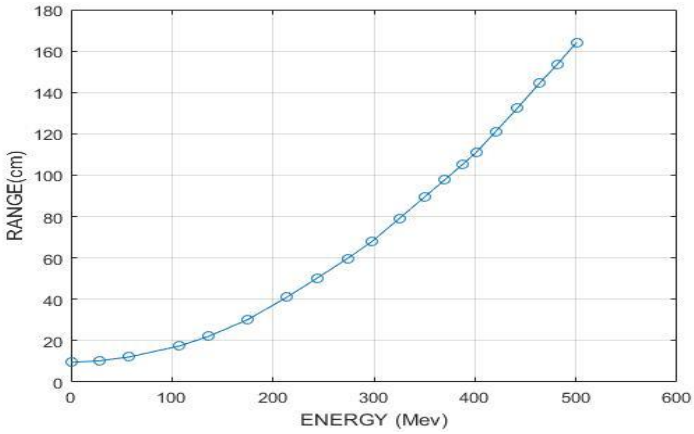

Figure 6. Range as function energies in Skin

Figure 6 shows an inverse relation for the stopping power of protons with their range. The stopping power was high at low proton energies, it indicated a large energy loss with a short range distance. Furthermore, as the proton energy increases, the stopping power decreases and the stopping range in the continuous hysteresis approximation (CSDA) increases. Overall, the results confirmed the important role of proton energy in determined the amount of energy within range in tissues.Calculating stopping power, along with continuous stopping range CSDA range values, can be a useful tool to understand how protons are transported and their energy is deposited in tissues, and this data can contribute to studies relative to proton radiation therapy.

4. Discussion

The present study provides a theoretical analysis of proton electronic stopping power and continuous slowing down approximation (CSDA) range in human intestine, larynx, and skin tissues using the Hartree–Fock–Roothaan approach. The findings demonstrate a consistent energy-dependent relationship between proton stopping power and penetration range across the investigated biological tissues. In general, electronic stopping power decreases as incident proton energy increases, whereas the CSDA range exhibits an increasing trend. This behavior is consistent with the fundamental principles of charged-particle interactions with matter, in which energy transfer through excitation and ionization depends on projectile velocity and the electronic properties of the target material. These findings are in line with the theoretical investigations of Usta and Tufan [3] and the fundamental stopping-power formulations discussed by Salvat [16], emphasizing the importance of electronic structure and projectile energy in determining proton energy-loss characteristics.

The results obtained for intestinal tissue reveal a substantial reduction in electronic stopping power over the investigated proton energy interval. The stopping power decreases from 207.294 MeV·cm²/g at 1.007 MeV to 4.711 MeV·cm²/g at 126.579 MeV, reaching 0.567 MeV·cm²/g at 678.672 MeV. Conversely, the calculated CSDA range increases from 2.31 cm at 50 MeV to 31.8 cm at 206 MeV, indicating a greater penetration capability at higher incident energies. This contrasting behavior reflects the relationship between proton velocity, electronic interactions, and the cumulative energy loss experienced during transport through biological matter. The calculated trends are consistent with the theoretical basis of proton range estimation described by Newhauser and Zhang [24], in which proton penetration depth depends strongly on initial kinetic energy and the stopping properties of the traversed medium.

A similar pattern is observed in laryngeal tissue, where the electronic stopping power decreases from 207.303 MeV·cm²/g at 1 MeV to 1.591 MeV·cm²/g at 461.266 MeV. The relatively high stopping-power values at lower incident energies suggest that slower protons undergo more intensive interactions with the target electrons, resulting in greater energy loss per unit mass thickness. As proton energy increases, the stopping power decreases because the energy-transfer process becomes less pronounced along a given

path length. The CSDA calculations also indicate increasing penetration distances with increasing proton energy, although the corresponding range values require careful evaluation of the energy–range correspondence reported in Table 2. These findings support the general physical interpretation that proton transport is governed by both incident particle energy and the electronic characteristics of the target tissue. Similar considerations have been emphasized in previous theoretical and computational investigations of proton interactions with biological targets [2].

The analysis of skin tissue further supports the energy-dependent behavior observed in the intestinal and laryngeal samples. Electronic stopping power decreases from 209.831 MeV·cm²/g at 1.001 MeV to 1.029 MeV·cm²/g at 682.464 MeV. Meanwhile, the reported CSDA range increases from 9.524 cm to 164.149 cm over the tabulated range-energy interval. The overall tendency indicates that high-energy protons possess greater penetration capability, whereas lower-energy protons exhibit higher energy loss per unit mass thickness. Although the three investigated tissues demonstrate broadly similar stopping-power trends, their distinct biological compositions and electronic characteristics may influence their quantitative energy-loss behavior. However, direct conclusions regarding tissue-specific differences require comparison at identical proton energies using consistent material-density and elemental-composition parameters. These considerations are important because proton stopping properties are determined not only by projectile energy but also by the physical and chemical properties of the absorbing medium [3], [10].

From a theoretical perspective, the application of Hartree–Fock–Roothaan wave functions provides an atomic-level framework for representing the electronic structure involved in proton–matter interactions. The use of Slater-type orbital expansions allows electron-density information to be incorporated into the calculation of effective excitation parameters and electronic stopping behavior. This approach is supported by the atomic wave-function methodology developed by Bunge et al. [23], which provides a mathematical basis for describing electronic distributions in atoms. Incorporating electronic-structure considerations is particularly relevant when evaluating interactions in biological materials containing multiple atomic constituents. Nevertheless, the accuracy of the theoretical predictions depends on the assumptions used to represent the tissue composition, excitation energies, and energy-loss mechanisms.

The findings also have potential implications for proton radiation applications, particularly in understanding energy deposition and penetration behavior in biological tissues. In proton therapy, accurate knowledge of stopping power and proton range is essential for estimating the depth at which radiation energy is deposited and for reducing unnecessary exposure to surrounding healthy tissues. The calculated energy-dependent trends provide preliminary theoretical information that may contribute to the development and evaluation of proton transport models. Previous studies have emphasized the importance of proton range estimation and radiation interaction modeling for improving treatment precision and understanding the physical basis of particle therapy [11], [12]. However, the present calculations should be interpreted as theoretical estimates rather than direct evidence of clinical dosimetric accuracy, since treatment planning requires additional consideration of tissue heterogeneity, nuclear interactions, beam characteristics, and patient-specific anatomical conditions.

Several limitations should be considered when interpreting these findings. First, the investigation is theoretical and does not include experimental measurements or independent validation against established proton stopping-power databases. Second, the CSDA approach assumes continuous average energy loss and does not explicitly account for stochastic energy-loss fluctuations, range straggling, or lateral scattering. Third, the reported numerical data contain certain inconsistencies in the correspondence between proton energy and CSDA range, particularly in the laryngeal and skin tissue tables, which should be resolved before quantitative comparisons are made. Moreover, potential variations in tissue composition, density, and physiological characteristics were not systematically evaluated. Future research should therefore incorporate experimentally validated material properties, comparisons with reference stopping-power datasets, and

Monte Carlo particle-transport simulations to assess the reliability of the predicted ranges and energy-deposition patterns. Such investigations would strengthen the applicability of the Hartree–Fock–Roothaan approach to biomedical radiation physics and proton therapy modeling.

Overall, the theoretical findings demonstrate that incident proton energy is a major determinant of electronic stopping power and CSDA penetration range in human intestine, larynx, and skin tissues. The observed decrease in stopping power and increase in penetration range with increasing proton energy provide a consistent qualitative description of proton transport behavior in the investigated biological media. By incorporating atomic electronic-structure considerations into stopping-power calculations, the present study contributes to the theoretical understanding of proton interactions with biological tissues. Further validation and refinement of the computational framework are necessary before these results can be applied to quantitative radiation dosimetry or clinical proton therapy planning.

5. Conclusion

In conclussion, electronic stopping power and CSDA range of protons in intestine, larynx, and skin tissues have been investigated over a protons energy . The results revealed the characteristics of proton energy loss and range behavior in three types of tissue. he stopping power calculation decreased with increased proton energy and vice versa . High stopping power observes at low energies of protons , indicated great energy losses . However, the CSDA range increased with increased proton energy, demonstrated that higher energies protons penetrats deeper into tissues before losing energy. The observed results established inversely propotional of proton stopping power with range. Furthermore, the toping power studies of intestine, larynx, and skin tissues provided a foundemental to investigate the effective of tissue as well as density on proton energy-loss processes and range characteristics. Overall, the results emphasized an importance of proton energies and tissue properties to determine energy deposition and range depth. These results have provided useful tools and knowledge for understanding proton interactions with tissues, and will support future studies on proton transport and radiation dose measurement in tissues.

REFERENCES

[1]M. O. El-Ghossain,Calculations Of Stopping Power, And Range Of Electrons Interaction With Different Material And Human Body Parts,INTERNATIONAL JOURNAL OF SCIENTIFIC & TECHNOLOGY RESEARCH VOLUME 6, ISSUE 01, JANUARY 2017 ISSN 2277-8616 114 IJSTR©2017 www.ijstr.org .

[2]Camila Strubbia Mangiarelli , Verónica B. Tessaro , Michaël Beuve and Mariel E. Galassi ,Proton Interactions with Biological Targets: Inelastic Cross Sections, Stopping Power, and Range Calculations,Atoms2025, 13(10), 83;https://doi.org/10.3390/atoms13100083

[3]Metin Usta , Mustafa Çağatay Tufan,Stopping power and range calculations in human tissues by using the Hartree-Fock-Roothaan wave functions,Radiation Physics and Chemistry, 2017, 43-50,Vol.140

[4] Fred A. Mettler, Jr., M.D. and Arthur C. Upton, M.D. Medical Effects of Ionizing Radiation, Grune & Stratton, Inc., Orlando, Florida, 1995

[5]Sgouros, G., Hobbs, R., & Josefsson, A. (2018). Dosimetry and radiobiology of alpha-particle emitting radionuclides. Current Radiopharmaceuticals, 11(3), 209–214. https://doi.org/10.2174/1874471011666180426130058

[6]Zaid M. Nuri1, Abdulla Z. Nuri2, Dheyab T. Noori3, Sabah Mahmoud Aman Allah,Comparison of The Stopping Power of the Proton and Alpha Particle in Some Elements,CENTRAL ASIAN JOURNAL OF MEDICAL AND NATURAL SCIENCES https://cajmns.casjournal.org/index.php/CAJMNS Volume: 07 Issue: 04 | October 2026 ISSN: 2660-4159

[7]Chang-kai Li, Fei Mao, Feng Wang, Yan-long Fu, Xiao-ping Ouyang6, and Feng-Shou Zhang ,Electronic stopping power of slow-light channeling ions in ZnTe from first principles,Phys. Rev. A 95, 052706 – , 2017.DOI: https://doi.org/10.1103/PhysRevA.95.052706

[8]Alfredo A. Correa,Calculating electronic stopping power in materials from first principles,Computational Materials Science, 2018, 291-303,Vol, 150.
[9] Tan, Z., & Xia, Y. (2012). Stopping power and mean free path for low-energy electrons in ten scintillators over energy range of 20–20,000 eV. Applied Radiation and Isotopes, 70(1), 296–300.
[10]Amandeep Sharma , Poonamjot , Simranpreet Kaur ,Radiological Characterization of Tissue Equivalent Materials: A Computational Approach,J Med Phys. 2026 Mar 31;51(1):118–128. doi: 10.4103/jmp.jmp_233_25.
[11]Julius Werner , Francesco Pennazio , Niklas Schmid , Elisa Fiorina , Davide Bersani , Piergiorgio Cerello , Jona Kasprzak , Nicola Mosco , Sahar Ranjbar , Roberto Sacchi , Veronica Ferrero , Magdalena Rafecas ,Stopping power and range estimations in proton therapy based on prompt gamma timing: motion models and automated parameter optimization,Phys Med Biol. 2024 ,15;69(14). doi: 10.1088/1361-6560/ad5d4b.
[12]Durante, M., & Paganetti, H. (2016). Nuclear physics in particle therapy: A review. Reports on Progress in Physics, 79(9), 096702. https://doi.org/10.1088/0034-4885/79/9/096702
[13]Spyridon A Kalospyros , Angeliki Gkikoudi , Athanasios Koutsostathis , Athanasia Adamopoulou , Spyridon N Vasilopoulos , Vasileios Rangos , Erato Stylianou-Markidou , Ioannis Pantalos , Constantinos Koumenis , Alexandros G Georgakilas ,Radiobiological and Clinical Advantages of Proton Therapy in Modern Cancer Treatment,Cancers (Basel). 2026 Mar 9;18(5):885. doi: 10.3390/cancers18050885
[14]Zhirong Sun ,Editors: Rui Jiang , Xuegong Zhang , Michael Q Zhang,Foundations for the Study of Structure and Function of Proteins,Basics of Bioinformatics. 2013 Jul 1:303–336. doi: 10.1007/978-3-642-38951-1_10
[15]Casas, D., Barriga-Carrasco, M. D., Rubio, J., & Morales, R. (2014). Energy loss of protons and He^{2+} beams in plasmas. Global NEST Journal, 16(6), 1085–1090. https://doi.org/10.30955/gnj.00135
[16]Salvat, F. (2022). Bethe stopping-power formula and its corrections. Physical Review A, 106(3), 032809. https://doi.org/10.1103/PhysRevA.106.032809
[17] N. Tsoulfanidis and S. Landsberger, Measurement and Detection of Radiation, 5th ed. Boca Raton, FL, USA: CRC Press, 2021.
[18]Amandeep Sharma , Poonamjot , Simranpreet Kaur ,Radiological Characterization of Tissue Equivalent Materials: A Computational Approach,J Med Phys. 2026 Mar 31;51(1):118–128. doi: 10.4103/jmp.jmp_233_25.
[19]Julius Werner , Francesco Pennazio , Niklas Schmid , Elisa Fiorina , Davide Bersani , Piergiorgio Cerello , Jona Kasprzak , Nicola Mosco , Sahar Ranjbar , Roberto Sacchi , Veronica Ferrero , Magdalena Rafecas ,Stopping power and range estimations in proton therapy based on prompt gamma timing: motion models and automated parameter optimization,Phys Med Biol. 2024 ,15;69(14). doi: 10.1088/1361-6560/ad5d4b.
[20] Giri, K.; Rupa K. Energy loss of proton beam on ovary tumor. Journal of Nepal Physical Society 2019, 1, 24-29. https://doi.org/10.3126/jnphyssoc.v5i1.26879
[21]Durante, M., & Paganetti, H. (2016). Nuclear physics in particle therapy: A review. Reports on Progress in Physics, 79(9), 096702. https://doi.org/10.1088/0034-4885/79/9/096702
[22]Spyridon A Kalospyros , Angeliki Gkikoudi , Athanasios Koutsostathis , Athanasia Adamopoulou , Spyridon N Vasilopoulos , Vasileios Rangos , Erato Stylianou-Markidou , Ioannis Pantalos , Constantinos Koumenis , Alexandros G Georgakilas ,Radiobiological and Clinical Advantages of Proton Therapy in Modern Cancer Treatment,Cancers (Basel). 2026 Mar 9;18(5):885. doi: 10.3390/cancers18050885
[23] Bunge, C.F., Barrientos, J.A., Bunge, A.V., 1993. Roothaan-Hartree-Fock ground-state atomic wave functions: Slater-type orbital expansions and expectation values for Z=2-54. At. Data Nucl. Data Tables 53, 113–162.
[24]Wayne D Newhauser and Rui Zhang, The physics of proton therapy,Phys Med Biol. 2015 April 21; 60(8): R155–R209. doi:10.1088/0031-9155/60/8/R155.
[25]Paganetti, H. (2015). Physics of proton therapy. Physics in Medicine & Biology, 60(8), R155–R209. https://doi.org/10.1088/0031-9155/60/8/R155